Chemical Science

EDGE ARTICLE

View Article Online
View Journal | View Issue

Open Access Article. Published on 09 April 2018. Downloaded on 1/10/2026 7:20:06 AM.
This article is licensed under a Creative Commons Attribution-NonCommercial 3.0 Unported Licence.

Check for updates

Cite this: *Chem. Sci.*, 2018, **9**, 4444

9,10-Azaboraphenanthrene-containing small molecules and conjugated polymers: synthesis and their application in chemodosimeters for the ratiometric detection of fluoride ions†

Weidong Zhang,[a] Guoping Li,[a] Letian Xu,[a] Yue Zhuo,[a] Wenming Wan,[b] Ni Yan[c] and Gang He*[a]

Received 10th February 2018
Accepted 6th April 2018

DOI: 10.1039/c8sc00688a

rsc.li/chemical-science

The introduction of main group elements into conjugated scaffolds is emerging as a key route to novel optoelectronic materials. Herein, an efficient and versatile way to synthesize polymerizable 9,10-azaboraphenanthrene (**BNP**)-containing monomers by aromaticity-driven ring expansion reactions between highly antiaromatic borafluorene and azides is reported, and the corresponding conjugated small molecules and polymers are developed as well. The **BNP**-containing small molecules and conjugated polymers showed good air/moisture stability and notable fluorescence properties. Addition of fluoride ions to the **BNP**-based small molecules and polymers induced a rapid change in the emission color from blue to green/yellow, respectively, accompanied by strong intensity changes. The conjugated polymers showed better ratiometric sensing performance than small molecules due to the exciton migration along the conjugated chains. Further experiments showed that the sensing process is fully reversible. The films prepared by solution-deposition of **BNP**-based compounds in the presence of polycaprolactone also showed good ratiometric sensing for fluoride ions.

1 Introduction

The fluoride anion (F^-) has recently received well-deserved attention from the scientific community not only because of its importance in many fields of human activities, including toothpaste, vitamins, and dietary supplements but also because of its effect on the environment.[1–4] As a result, many optical sensors have been developed for detecting F^-. The construction strategies are generally based on the strong molecular interactions between sensors and F^-, including H-bonding, F^--mediated chemical reactions and Lewis acid–base interactions. However, sensors based on hydrogen bonding[5–10] and chemical reactions[11,12] suffer from several drawbacks, such as a false positive signal or low sensitivity and long response time. In contrast, sensors based on the interactions between fluoride ions and Lewis acids have been regularly employed for the sensing of fluoride ions due to their superior sensitivity, simplicity, and reversibility.

As a class of typical Lewis acids, organoboranes with intrinsic Lewis acidity can react with fluoride to afford fluoroborate anions efficiently.[13–17] This reaction is traditionally described as an addition reaction, which takes advantage of the extended π-conjugation in tricoordinate organoboranes with the p-orbital of the boron center that can accept an electron pair from F^-. However, a large number of organoboranes are air- and moisture-sensitive; thus, improving their air stability is a very important research topic in this field. A common strategy to construct stable organoboranes involves introducing a bulky aryl group onto the boron atom, but this method is challenging because of the tough synthesis, especially for boroles.[18–22]

Replacing the boron atom by a boron–nitrogen (BN) unit in aromatics has been demonstrated to be an alternative way to stabilize organoboranes (boroles). The BN derivatives not only display high stability and excellent luminescence properties[23–26] but also show Lewis acidity on the boron center, which can easily react with Lewis bases, such as F^-. This property is explained by the existence of the p-orbital on boron atoms in BN-containing conjugated heterocycles. Since Dewar and co-workers pioneered the synthesis of BN isosteres of simple polycyclic aromatic hydrocarbons (PAHs) and their derivatives

[a]*Frontier Institute of Science and Technology jointly with School of Science, State Key Laboratory for Strength and Vibration of Mechanical Structures, Xi'an Key Laboratory of Sustainable Energy Materials Chemistry, Xi'an Jiaotong University, Xi'an, Shaanxi 710054, China. E-mail: ganghe@mail.xjtu.edu.cn*

[b]*Centre for Bioengineering and Biotechnology, China University of Petroleum (East China), Qingdao, Shandong 266580, China*

[c]*Polymer Materials & Engineering Department, Institute of Polymer Materials, School of Materials Science & Engineering, Chang'an University, Xi'an, Shaanxi 710064, China*

† Electronic supplementary information (ESI) available: Experimental details, NMR spectra of all the new compounds, crystallographic data and results of theoretical calculations. CCDC 1818909. For ESI and crystallographic data in CIF or other electronic format see DOI: 10.1039/c8sc00688a

This journal is © The Royal Society of Chemistry 2018

Open Access Article. Published on 09 April 2018. Downloaded on 1/10/2026 7:20:06 AM.
This article is licensed under a Creative Commons Attribution-NonCommercial 3.0 Unported Licence.

in the 1960s, significant attention has been focused on this type of chemistry[27,28] and fascinating BN derivatives have recently been developed by Liu,[29,30] Jäkle,[31,32] Braunschweig[33,34] and other groups.[35–37] Very recently, five-membered, unsaturated and highly antiaromatic boroles[38] have been proven to react *via* 1,1- and 1,2-insertion reactions with a variety of substrates, such as carbon monoxide, alkynes and isocyanides, as well as with a ketone or an aldehyde to generate a number of aromatic six- or seven-membered heterocycles, which are not available by other methods.[39–42] Interestingly, the efficient aromaticity-driven ring-opening strategy, first developed by Braunschweig's group, was also used by Martin's group to synthesize the desired BN derivatives with high yield through the reaction between boroles and azides.[43–45] However, synthesis of novel BN-containing conjugated heterocycles through the ring-opening reaction is still rare. Evidently, exploring the scope of the ring-opening reaction to obtain new BN-containing molecules and extending the family of BN moiety-containing conjugated polymers is not only important for BN and polymer chemistry, but also meaningful for F^- sensing and other optoelectronic applications.

Based on these considerations, herein, for the first time, we report a new strategy to synthesize polymerizable 9,10-azaboraphenanthrene (**BNP**)-based monomers by the aromaticity-driven ring-opening reaction between a borafluorene precursor and an azide, as well as the respective **BNP**-containing conjugated polymers (Scheme 1). Because of the existence of the p-orbital on boron atoms, these small molecules and polymers were successfully used as chemodosimeters for the ratiometric detection of F^- with high selectivity and sensitivity.

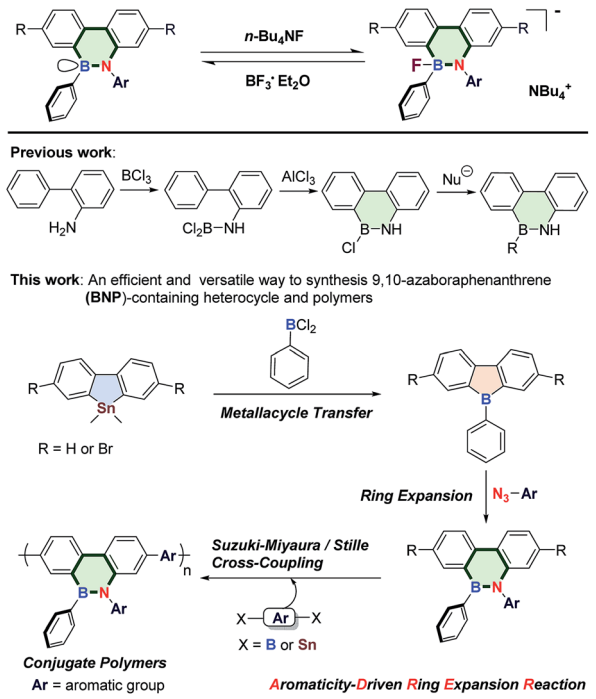

Scheme 1 Aromaticity-driven ring expansion route to 9,10-azaboraphenanthrene-containing conjugated small molecules and polymers.

2 Results and discussion

2.1. Synthesis of BNP-containing small molecules and polymers

The highly antiaromatic borafluorene precursors **3** and **4** (NICS(1)zz: +26.0 for **3** and +24.8 for **4**, Table S3†) were synthesized through boron–tin exchange reactions and were directly used for the ring-opening reactions without further separation and purification. The ring-opening reaction between borafluorene precursors (**3** and **4**) and 2-azido-1,3,5-trimethyl-benzene gave the desired aromatic **BNP** derivatives **5** and **6** (NICS(1)zz: −6.9 for **5** and −6.6 for **6**, Table S3†) with 50% and 71% yield, respectively (Scheme 2). The successful synthesis of **5**/**6** was confirmed by multinuclear NMR, high-resolution mass spectrometry (HRMS), and elemental analysis (EA) (ESI†). The white crystals of **6** were obtained from saturated hexanes/CH_2Cl_2 mixtures, and were further analyzed by single-crystal X-ray crystallography. As shown in Fig. 1, the core rings of compound **6** had an almost planar conformation, and the B–N distance was 1.414(5) Å (*i.e.* this distance is shorter than the reported BN bond distances of (*E*)-2-mesityl-1-(2,6-dibromo-4-methylphenyldiazenyl)-3,4,5,6-tetraphenyl-1,2-azaborinine (1.443 Å)[44,45] and (*E*)-6-phenyl-5-(phenyldiazenyl)-5,6-dihydrodibenzo[*c*,*e*]-[1,2]azaborinine (1.426 Å),[46] Table S2†). The bond angles (deg) of N(1)–B(1)–C(1), N(1)–B(1)–C(14) and C(1)–B(1)–C(14) were 116.0(3)°, 121.8(3)° and 122.2(3)°, respectively, indicating a distorted trigonal planar environment around the boron center as expected for a B–N stable system. The mechanism of borole ring expansion by azides was revealed carefully by using experimental and theoretical methods by Martin and co-workers.[43] According to this mechanism, the α-nitrogen of azide coordinates with the

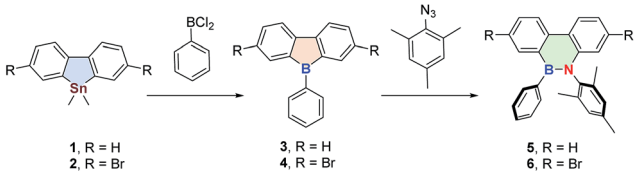

Scheme 2 Synthesis of BNP derivatives **5** and **6**.

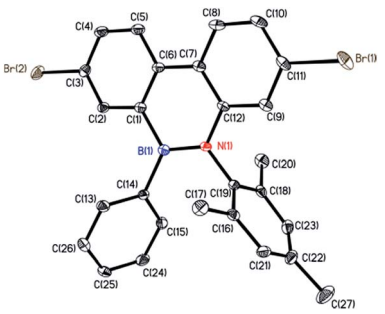

Fig. 1 X-ray crystal structure of **6**. Selected bond lengths (Å): N(1)–C(12), 1.412(4); N(1)–B(1), 1.414(5); N(1)–C(19), 1.452(5); B(1)–C(1), 1.551(6); and B(1)–C(14), 1.576(5). Bond angles (deg): C(12)–N(1)–B(1), 123.2(3); C(12)–N(1)–C(19), 116.1(3); B(1)–N(1)–C(19), 120.7(3); N(1)–B(1)–C(1), 116.0(3); N(1)–B(1)–C(14), 121.8(3); and C(1)–B(1)–C(14), 122.2(3).

Open Access Article. Published on 09 April 2018. Downloaded on 1/10/2026 7:20:06 AM. This article is licensed under a Creative Commons Attribution-NonCommercial 3.0 Unported Licence.

empty p orbital of the boron atom, followed by rearrangement to a bicyclic intermediate and generation of a kinetically favoured eight-membered heterocycle; alternatively molecular N_2 is released to form the thermodynamically favoured **BNP** derivatives (Fig. S1†).

Given the successful synthesis of **5** and **6**, we were eager to explore Suzuki–Miyaura and Stille cross-coupling methodologies to extend the π-conjugation of these systems (Scheme 3). Firstly, model compound **8** was synthesized as a white solid in 52% yield by a Suzuki–Miyaura coupling reaction between monomer **6** and 4-methylphenylboronic acid (**7**), using $Pd(PPh_3)_4$ as a catalyst and Aliquat-336 as a phase-transfer agent. Similarly, the conjugated polymer **P1** with a number-average molecular weight (M_n) of 6.17 kg mol^{-1} (PDI = 1.52, Fig. S3†) was successfully prepared by a Suzuki–Miyaura coupling reaction between **6** and 2,2′-(9,9-didecyl-9*H*-fluorene-2,7-diyl)bis(4,4,5,5-tetramethyl-1,3,2-dioxaborolane) (**9**). Moreover, monomer **6** was also tolerated under the reaction conditions of the Stille-coupling, and regiorandom polymer **P2** (M_n of 6.08 kg mol^{-1} and PDI = 1.32, Fig. S4†) was successfully obtained through a reaction between **6** and (3-hexylthiophene-2,5-diyl)bis(tributylstannane) (**10**). The integrity of the 9,10-azaboraphenanthrene azaborine moieties in **P1** and **P2** was confirmed by broad signals in the ^{11}B NMR spectra at δ = 34.0 ppm for **P1** and δ = 33.7 ppm for **P2**, which were close to those of the monomers. Polymers **P1** and **P2** are soluble in typical organic solvents of medium polarity, such as DMF, THF, toluene, CH_2Cl_2 and $CHCl_3$, which can be readily processed into thin films *via* a spin-coating method for future applications.

2.2. Photophysical properties of the BNP-containing small molecules and polymers

Phenanthrene is a well-known fluorophore and is widely used as a conjugated component in luminescent organic materials.[47–50] In comparison with the photophysical and electrochemical properties of phenanthrene, a BN–phenanthrene-containing heterocycle provided a clear-cut view of the characteristic properties.[51,52] The lowest-energy absorption peaks of **5** showed major absorption bands at λ_{max} = 317 and 329 nm, while its emission was observed at $\lambda_{max,em}$ = 355 nm (Fig. S5†). Due to its extended π-conjugation, the absorption and emission spectra of **8** showed maxima at 340 nm and 391 nm, respectively, which were slightly bathochromically shifted compared to **5** (Fig. S7†). The lowest energy absorption bands in **5** and **8** were attributed to lower symmetry in the heterocycle *vs.* the phenyl ring.[53,54] The fluorescence spectra of **5** and **8** exhibited emission features with similar lifetimes (τ = 3.1 ns for **5** and 2.2 ns for **8**) and high quantum yields (Φ = 0.52 for **5** and 0.77 for **8**). In comparison to **5** and **8**, polymers **P1** and **P2** exhibited a notable red-shift in UV-vis absorption and fluorescence spectra as a result of their increased aromatic chain linkage. While **P1** showed the maximum absorption at λ_{max} = 377 nm, **P2** absorbed at λ_{max} = 399 nm, the latter being *ca.* 20 nm red-shifted compared with **P1**. When excited at λ_{ex} = 350 nm, polymers **P1** and **P2** displayed blue fluorescence at $\lambda_{max,em}$ = 414 (**P1**) and 458 nm (**P2**). However, the quantum yield of **P1** (Φ = 0.88) is about 1.5-fold higher than that of **P2** (Φ = 0.57).

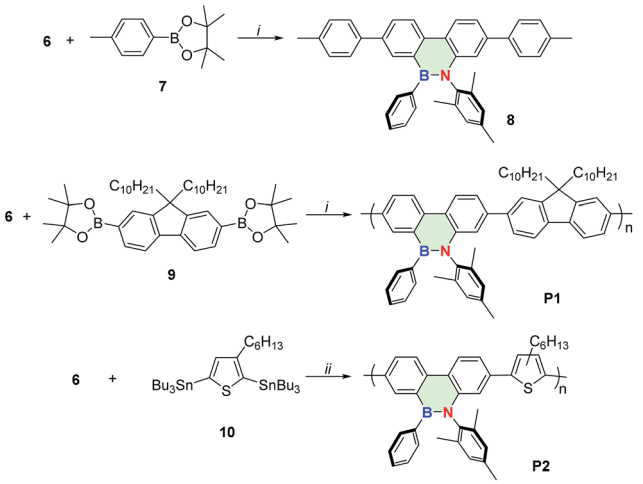

Scheme 3 Synthesis of the BNP-containing molecule **8** and polymers **P1** and **P2** by the Suzuki–Miyaura or Stille cross-coupling.

2.3. Redox properties of the 9,10-azaboraphenanthrene-containing small molecules and polymers

The electron-acceptor properties of the small molecules and polymers were studied by cyclic voltammetry in DCM solution in a glovebox. As shown in Fig. S17,† an irreversible oxidation at around +0.4 to +1.0 V *vs.* Fc/Fc^+ was found for the **BNP**-containing small molecules and polymers (**5**, $E_{1/2}$ = 0.95 V; **8**, $E_{1/2}$ = 0.84 V; **P1**, $E_{1/2}$ = 0.47 V; and **P2**, $E_{1/2}$ = 0.44 V). Accordingly, the highest occupied molecular orbital (HOMO) energy levels of **5**, **8**, **P1** and **P2** were determined to be −5.75 eV, −5.64 eV, −5.27 eV and −5.24 eV, respectively; these data are consistent with the relationship between the extension of the π-conjugation and the increase in HOMO energy levels. The LUMO levels, calculated from the HOMO levels and the optical band gaps (**5**, 3.69 eV; **8**, 3.39 eV; **P1**, 3.04 eV; and **P2**, 2.85 eV), were *ca.* −2.06, −2.25, −2.23 and −2.39 eV (Fig. 2), which are in good accordance with the calculation results (Table S4 and Fig. S18–S21,† calculated in the gas phase; Fig. S22–S25,† calculated in DCM). Compared to boroles,[22,55] the redox waves of boron–nitrogen (BN) units showed significant differences, implying that BN substitution changed the electronic structure of the compound significantly. Notably, both B and N atoms contribute to the molecular orbitals to a large extent, thus being responsible for the altered electronic properties.

2.4. Ratiometric fluoride-ion sensing properties of the BNP-containing small molecules and polymers

Owing to the presence of the empty p-orbital, tricoordinate organoboranes are known to accommodate a lone pair of electrons from a Lewis base, which will strongly change the optoelectronic properties. Based on this mechanism, many optical sensors for F^- ions were developed. Considering the existence of the p-orbital on boron in the **BNP**-containing small molecules

Open Access Article. Published on 09 April 2018. Downloaded on 1/10/2026 7:20:06 AM.
This article is licensed under a Creative Commons Attribution-NonCommercial 3.0 Unported Licence.

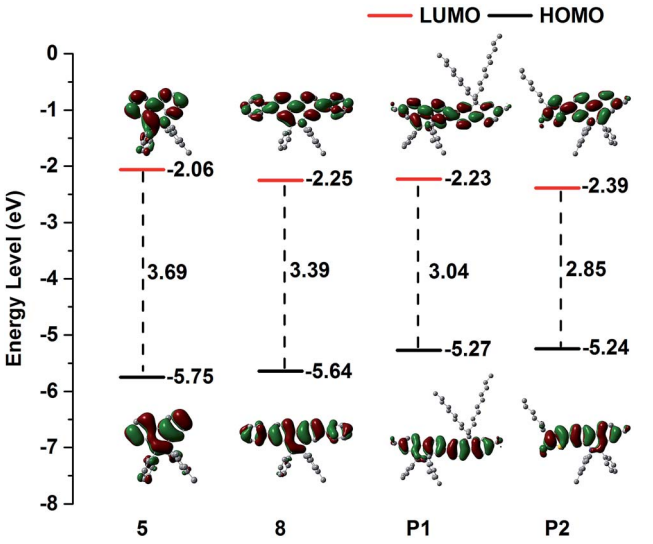

Fig. 2 Experimental orbital energy levels and HOMO/LUMO orbital plots of **5**, **8**, **P1** and **P2**.

and polymers, we decided to investigate the response of these compounds to fluoride anions by UV-vis and fluorescence titration experiments, which were carried out using a solution of *n*-tetrabutylammonium fluoride (TBAF). Changes in the absorptions and fluorescence spectra of compounds **5**, **8**, **P1** and **P2** were compared in THF (Fig. 3). Upon addition of aliquots of fluoride to a solution of **5**, a gradual decrease in intensity of the absorption bands at $\lambda = 317$ nm and 329 nm was observed, and a gradually increasing red-shift at $\lambda = 372$ nm was observed as a result of the binding of fluoride to the boron atom of the BN moiety (Fig. 3a). Similarly, fluoride addition to **8** led to a new absorption band at $\lambda = 411$ nm, which was a red-shifted by *ca.* 39 nm relative to the maximum absorption observed in **5** (Fig. 3c). These phenomena were well supported by the calculation results (Fig. S6 and S8†). Titration of **5** and **8** with F^- was monitored by fluorescence spectroscopy. As shown in Fig. 3b, compound **5** exhibits an emission maximum at 355 nm, while the emission maximum gradually decreased and the new emission peak at around 448 nm increased in intensity after the addition of F^- and a well-defined isoemission point at 410 nm was observed, which revealed the formation of new species. Compound **8** showed similar results (Fig. 3d), but the emission color changed from blue to green after the titration (λ_{em} = 391 nm to 498 nm) with an isoemission point at $\lambda = 452$ nm. The polymers also exhibited almost identical titration features; **P1** and **P2** were titrated with TBAF in THF and monitored by UV-vis absorption (Fig. 3e and g) and fluorescence spectroscopy (Fig. 3f and h). Upon binding of F^-, the bands in the UV-vis spectra of **P1** (λ_{max} = 379 nm) and **P2** (λ_{max} = 399 nm) were gradually quenched and new absorption peaks emerged at λ = 436 nm and λ = 446 nm, respectively. For the fluorescence spectra, a similar phenomenon was observed; the emission of **P1** (λ_{em} = 414 nm) and **P2** (λ_{em} = 458 nm) was gradually quenched and a more red-shifted emission appeared at λ_{em} = 516 and 541 nm, respectively. We calculated the F^- binding

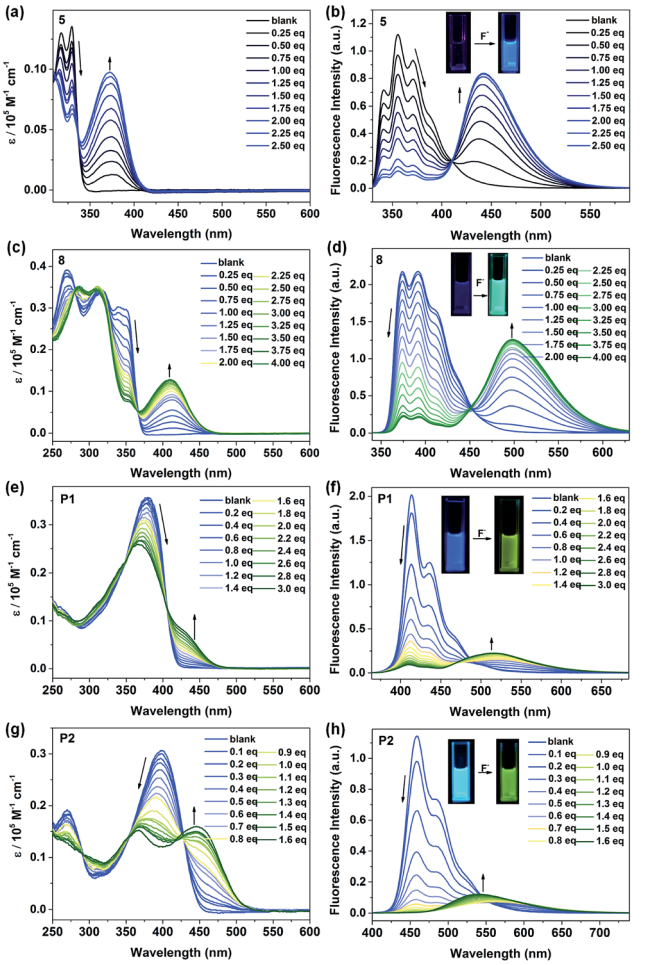

Fig. 3 Spectral changes in the UV/vis absorption (left) and fluorescence (right) after the addition of TBAF. (a and b) **5**, λ_{ex} = 300 nm, [**5**] = 10 μM; (c and d) **8**, λ_{ex} = 300 nm, [**8**] = 10 μM; (e and f) **P1**, λ_{ex} = 350 nm, [**P1**] = 10 μM; and (g and h) **P2**, λ_{ex} = 365 nm, [**P2**] = 10 μM. [F^-] = 1 mM.

constant of **5**, **8**, **P1** and **P2** using the Benesi–Hilderbrand plots shown in Fig. S14 (ESI†). The binding constants were determined to be 1.38×10^4 M^{-1} (**5**), 1.41×10^4 M^{-1} (**8**), 1.76×10^5 M^{-1} (**P1**) and 1.60×10^5 M^{-1} (**P2**). The emission intensity ratio of **5** (I_{448}/I_{354}), **8** (I_{498}/I_{391}), **P1** (I_{516}/I_{414}) and **P2** (I_{541}/I_{458}) increased with increasing the concentration of F^- (Fig. S13†), which means that the **BNP**-containing small molecules and polymers can be used as colorimetric F^- sensors.

In contrast to **5**, the Stern–Volmer plots of polymer **P2** showed more efficient fluorescence quenching (Fig. 4). The enhanced quenching efficiency of the polymer is likely due to the exciton migration along the polymer chain to lower energy quenching sites that are generated upon F^- binding.[56] This phenomenon is also known as the "molecular wire effect" or "super-quenching effect" for conjugated polymer-based sensors.[57,58] In this case, however, the Stern–Volmer plots of **P2** displayed an upward curvature in the intensity change, which could be a result of the combination of dynamic quenching and static quenching. In this system, the main reason for the upward curvature is the formation of weakly or non-emissive lower-energy aggregates upon fluoride titration,

Open Access Article. Published on 09 April 2018. Downloaded on 1/10/2026 7:20:06 AM.
This article is licensed under a Creative Commons Attribution-NonCommercial 3.0 Unported Licence.

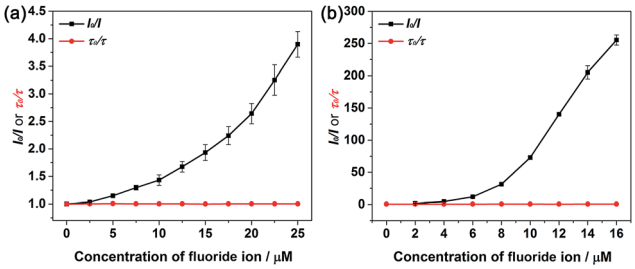

Fig. 4 Stern–Volmer plots of fluorescence intensity (I_0/I) and lifetime change (τ_0/τ) as a function of [F$^-$] of **5** (λ_{em} = 355 nm) (a) and **P2** (λ_{em} = 458 nm) (b) in THF upon addition of *n*-Bu$_4$NF.

which might contribute to the observed enhancement in fluorescence quenching.[56] Moreover, the fluorescence lifetimes and intensities of **5**, **8**, **P1** and **P2** were determined in the presence of different concentrations of F$^-$, and the results are shown in Fig. 4a and b, S15 and S16.† We observed that the lifetime curves were close to a straight line after adding F$^-$, indicating the static quenching nature of the sensing process.

The anion sensing properties of the **BNP**-containing small molecules and polymers were investigated upon simultaneous addition of a certain number of different anions. Fig. 5 shows the changes in the fluorescence spectra of **5**, **8**, **P1** and **P2** (1×10^{-5} M in THF) with 11 different anions, including F$^-$, Cl$^-$, Br$^-$, I$^-$, NO$_3^-$, ClO$_4^-$, BF$_4^-$, PF$_6^-$, AcO$^-$, H$_2$PO$_4^-$ and SO$_4^{2-}$. Specifically, upon the addition of F$^-$ to the solution of **5** and **8**, the fluorescence spectra showed distinct changes both in intensity and emission wavelength, while other anions showed almost no change in the fluorescence spectra. Similarly, it is evident that **P1** and **P2** bind F$^-$ selectively, whereas other anions do not show any affinity (except for AcO$^-$ and SO$_4^{2-}$ anions, which show a slight affinity for **P2**). The dramatic anion-specific response suggests that compounds **5**, **8**, **P1** and **P2** are highly selective colorimetric sensors for the detection of fluoride anions.

The electron-deficient boron atoms of BN–phenanthrene units are captured by the added F$^-$ leading to a change of geometry at boron centers. In order to gain further insight into the mechanism, the reversibility of the sensing performance of **5** was investigated by UV-vis and fluorescence spectroscopy. Evidently, the new product **5-F** can be converted back to the starting material, **5**, by treatment with a stronger fluoride scavenger such as BF$_3$·OEt$_2$ (Fig. 6). These results supported our assumption regarding the origin of BN–phenanthrene as a stable conformation without decomposition. To further explore this assumption, DFT calculations (Gaussian 09, B3LYP/6-31G*) were conducted. Geometry optimization of the possible isomers of **5** and **5-F** is shown in Fig. 6b. The calculated UV/Vis spectrum for **5-F** (Fig. S6†) indicates that the dominant absorption occurring at *ca.* 365 nm is in good agreement with the experimental results (*i.e.*, a major absorption band at 372 nm). The titrations were further verified by ^{19}F and ^{11}B NMR measurements. Upon addition of different equivalents of TBAF to compound **5**, a new signal appeared at −156.6 ppm in ^{19}F NMR (Fig. S37†) and 2.2 ppm in ^{11}B NMR spectra (Fig. S38†), indicating the formation of a fluoroborate complex (**5-F**). These results also demonstrated the potential of the present boron system as a new type of fluorescent sensor for the detection of the fluoride ion.[59]

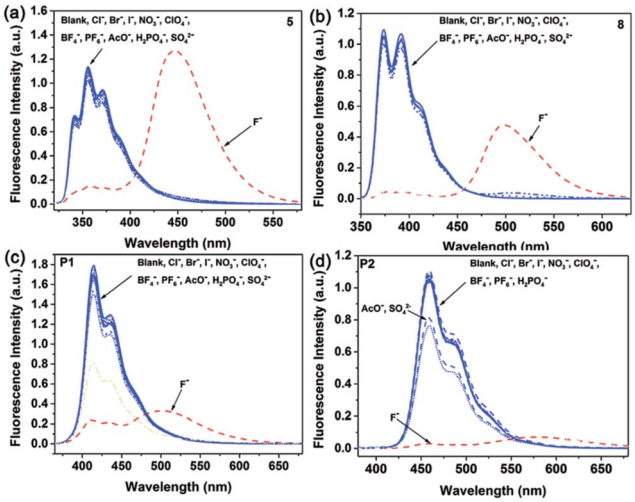

Fig. 5 (a–d) Complexation of **5**, **8**, **P1** and **P2** (1×10^{-5} M in THF) with different anions (THF, 5 equiv. of Bu$_4$N$^+$ salts, 0.01 M).

2.5. Application of the film sensors for fluoride ions

The **BNP**-containing small molecules and polymers can also be used to fabricate film sensors for F$^-$ (Fig. 7). Compounds **5** and **P2** were mixed with polycaprolactone (PCL) to prepare

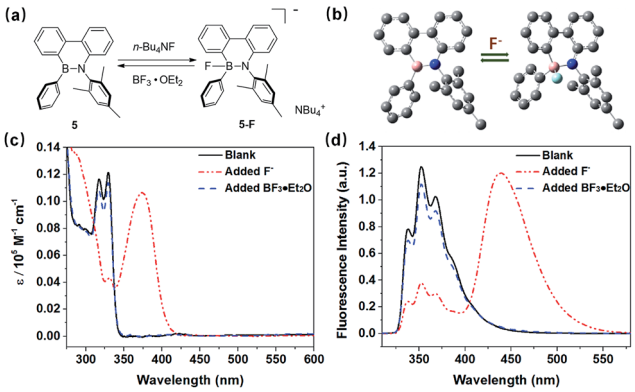

Fig. 6 (a) Proposed interaction of **5** with fluoride anions; (b) illustration of the predicted shape changes for **5** upon fluoride ion binding; and the absorption (c) and emission (d) spectra of **5** in THF (solid line) upon addition of fluoride ions (dashed-dotted line) and BF$_3$·OEt$_2$ (dashed line).

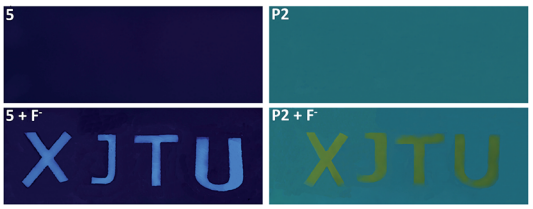

Fig. 7 The **5** and **P2**-based film sensors for fluoride anions under UV irradiation (λ_{ex} = 365 nm).

Open Access Article. Published on 09 April 2018. Downloaded on 1/10/2026 7:20:06 AM. This article is licensed under a Creative Commons Attribution-NonCommercial 3.0 Unported Licence.

a solution mixture (weight ratio: 1/400), which was further cast on a pre-cleaned glass substrate to fabricate the sensor films. The compound **5**-based film showed weak emission when irradiated with a hand-held UV lamp (λ_{ex} = 365 nm) at room temperature. However, a bright blue luminescence was observed upon writing the characters "XJTU" on the film using TBAF solution. Similarly, a blue-green luminescence was found for **P2** (λ_{ex} = 365 nm), and it immediately transformed into a yellow-green "XJTU" luminescence upon addition of fluoride ions. These findings are promising for advanced optoelectronic applications in solid-state sensing of F^- anions.

3 Conclusions

In summary, we have reported a highly efficient synthetic route for conjugated small molecules and polymers featuring 9,10-azaboraphenanthrene (**BNP**) units through aromaticity-driven ring-opening reactions. The **BNP**-containing conjugated small molecules and polymers showed good air and moisture stability as well as bright fluorescence properties; these compounds were used as effective and selective ratiometric sensors for F^- in THF solution among 11 anions (F^-, Cl^-, Br^-, I^-, NO_3^-, ClO_4^-, BF_4^-, PF_6^-, AcO^-, $H_2PO_4^-$, and SO_4^{2-}), resulting in dissimilar spectral changes from blue to green/yellow with different intensities, respectively. The large red shift in the absorption and the ratiometric fluorescence response are extremely desirable for the detection of F^-. Further experiments and DFT calculation results showed that the sensing process is fully reversible. Future work will involve extending this synthetic concept to incorporate hydrophilic moieties into **BNP** units to obtain a new sensing platform for the detection of fluoride anions in aqueous medium.

Conflicts of interest

There are no conflicts to declare.

Acknowledgements

We gratefully acknowledge financial support from the Natural Science Foundation of China (21603016 and 21704081), the Natural Science Foundation of Shaanxi Province (2017JQ2023), the Cyrus Chung Ying Tang Foundation and the National 1000-Plan program. We also thank Prof. Yu Fang for helpful discussions. We are especially grateful to Prof. Yanzhen Zheng for his help with X-ray crystallographic analysis. We thank Dr. Gang Chang and Yu Wang of the Instrument Analysis Center of Xi'an Jiaotong University for their assistance with acquiring photoluminescence (PL) spectra.

Notes and references

1 B. D. Gessner, M. Beller, J. P. Middaugh and G. M. Whitford, *N. Engl. J. Med.*, 1994, **330**, 95–99.
2 P. Singh, M. Barjatiya, S. Dhing, R. Bhatnagar, S. Kothari and V. Dhar, *Urol. Res.*, 2001, **29**, 238–244.
3 X. Zheng, W. Zhu, D. Liu, H. Ai, Y. Huang and Z. Lu, *ACS Appl. Mater. Interfaces*, 2014, **6**, 7996–8000.
4 P. A. Gale, *Acc. Chem. Res.*, 2006, **39**, 465–475.
5 P. A. Gale and C. Caltagirone, *Chem. Soc. Rev.*, 2015, **44**, 4212–4227.
6 Y. Zhou, J. F. Zhang and J. Yoon, *Chem. Rev.*, 2014, **114**, 5511–5571.
7 S. Ayoob and A. K. Gupta, *Crit. Rev. Environ. Sci. Technol.*, 2006, **36**, 433–487.
8 C. R. Wade, A. E. J. Broomsgrove, S. Aldridge and F. P. Gabbaï, *Chem. Rev.*, 2010, **110**, 3958–3984.
9 M. Cametti and K. Rissanen, *Chem. Soc. Rev.*, 2013, **42**, 2016–2038.
10 M. Cametti and K. Rissanen, *Chem. Commun.*, 2009, 2809–2829.
11 X.-F. Yang, H. Qi, L. Wang, Z. Su and G. Wang, *Talanta*, 2009, **80**, 92–97.
12 S. Y. Kim and J.-I. Hong, *Org. Lett.*, 2007, **9**, 3109–3112.
13 F. Cheng, E. M. Bonder and F. Jäkle, *J. Am. Chem. Soc.*, 2013, **135**, 17286–17289.
14 Z. Zhou, A. Wakamiya, T. Kushida and S. Yamaguchi, *J. Am. Chem. Soc.*, 2012, **134**, 4529–4532.
15 L. Trembleau, T. A. D. Smith and M. H. Abdelrahman, *Chem. Commun.*, 2013, **49**, 5850–5852.
16 G. Turkoglu, M. E. Cinar and T. Ozturk, *Eur. J. Org. Chem.*, 2017, 4552–4561.
17 Z. Li, H. Li, H. Xia, X. Ding, X. Luo, X. Liu and Y. Mu, *Chem.–Eur. J.*, 2015, **21**, 17355–17362.
18 F. Jäkle, *Chem. Rev.*, 2010, **110**, 3985–4022.
19 C. Fan, L. G. Mercier, W. E. Piers, H. M. Tuononen and M. Parvez, *J. Am. Chem. Soc.*, 2010, **132**, 9604–9606.
20 H. Braunschweig, R. D. Dewhurst and A. Schneider, *Chem. Rev.*, 2010, **110**, 3924–3957.
21 T. Kaese, A. Hübner, M. Bolte, H.-W. Lerner and M. Wagner, *J. Am. Chem. Soc.*, 2016, **138**, 6224–6233.
22 A. Iida and S. Yamaguchi, *J. Am. Chem. Soc.*, 2011, **133**, 6952–6955.
23 X.-Y. Wang, H.-R. Lin, T. Lei, D.-C. Yang, F.-D. Zhuang, J.-Y. Wang, S.-C. Yuan and J. Pei, *Angew. Chem., Int. Ed.*, 2013, **52**, 3117–3120.
24 R. Zhao, C. Dou, Z. Xie, J. Liu and L. Wang, *Angew. Chem., Int. Ed.*, 2016, **55**, 5313–5317.
25 X. Y. Wang, J. Y. Wang and J. Pei, *Chem.–Eur. J.*, 2015, **21**, 3528–3539.
26 G. Li, Y. Zhao, J. Li, J. Cao, J. Zhu, X. W. Sun and Q. Zhang, *J. Org. Chem.*, 2015, **80**, 196–203.
27 M. J. S. Dewar and W. H. Poesche, *J. Am. Chem. Soc.*, 1963, **85**, 2253–2256.
28 M. J. S. Dewar and P. M. Maitlis, *J. Am. Chem. Soc.*, 1961, **83**, 187–193.
29 A. W. Baggett, M. Vasiliu, B. Li, D. A. Dixon and S.-Y. Liu, *J. Am. Chem. Soc.*, 2015, **137**, 5536–5541.
30 P. G. Campbell, A. J. V. Marwitz and S.-Y. Liu, *Angew. Chem., Int. Ed.*, 2012, **51**, 6074–6092.
31 H. Kuhtz, F. Cheng, S. Schwedler, L. Boehling, A. Brockhinke, L. Weber, K. Parab and F. Jäkle, *ACS Macro Lett.*, 2012, **1**, 555–559.

Open Access Article. Published on 09 April 2018. Downloaded on 1/10/2026 7:20:06 AM.
This article is licensed under a Creative Commons Attribution-NonCommercial 3.0 Unported Licence.

32 K. Liu, R. A. Lalancette and F. Jäkle, *J. Am. Chem. Soc.*, 2017, **139**, 18170–18173.
33 H. Braunschweig, Q. Ye, M. A. Celik, R. D. Dewhurst and K. Radacki, *Angew. Chem., Int. Ed.*, 2015, **54**, 5065–5068.
34 M. Arrowsmith, H. Braunschweig, K. Radacki, T. Thiess and A. Turkin, *Chem.–Eur. J.*, 2017, **23**, 2179–2184.
35 M. Lepeltier, O. Lukoyanova, A. Jacobson, S. Jeeva and D. F. Perepichka, *Chem. Commun.*, 2010, **46**, 7007–7009.
36 J.-S. Lu, S.-B. Ko, N. R. Walters, Y. Kang, F. Sauriol and S. Wang, *Angew. Chem., Int. Ed.*, 2013, **52**, 4544–4548.
37 T. Hatakeyama, S. Hashimoto, S. Seki and M. Nakamura, *J. Am. Chem. Soc.*, 2011, **133**, 18614–18617.
38 W. Zhang, B. Zhang, D. Yu and G. He, *Sci. Bull.*, 2017, **62**, 899–900.
39 K. Huang and C. D. Martin, *Inorg. Chem.*, 2015, **54**, 1869–1875.
40 K. Huang, S. A. Couchman, D. J. D. Wilson, J. L. Dutton and C. D. Martin, *Inorg. Chem.*, 2015, **54**, 8957–8968.
41 A. Fukazawa, J. L. Dutton, C. Fan, L. G. Mercier, A. Y. Houghton, Q. Wu, W. E. Piers and M. Parvez, *Chem. Sci.*, 2012, **3**, 1814–1818.
42 C. Fan, W. E. Piers, M. Parvez and R. McDonald, *Organometallics*, 2010, **29**, 5132–5139.
43 S. A. Couchman, T. K. Thompson, D. J. D. Wilson, J. L. Dutton and C. D. Martin, *Chem. Commun.*, 2014, **50**, 11724–11726.
44 H. Braunschweig, C. Hoerl, L. Mailaender, K. Radacki and J. Wahler, *Chem.–Eur. J.*, 2014, **20**, 9858–9861.
45 H. Braunschweig, M. A. Celik, F. Hupp, I. Krummenacher and L. Mailaender, *Angew. Chem., Int. Ed.*, 2015, **54**, 6347–6351.
46 S. Yruegas, J. J. Martinez and C. D. Martin, *Chem. Commun.*, 2018, DOI: 10.1039/c8cc01529e.
47 H. Tian, J. Shi, S. Dong, D. Yan, L. Wang, Y. Geng and F. Wang, *Chem. Commun.*, 2006, 3498–34500.
48 H. Tian, J. Wang, J. Shi, D. Yan, L. Wang, Y. Geng and F. Wang, *J. Mater. Chem.*, 2005, **15**, 3026.
49 C. Yang, H. Scheiber, E. J. W. List, J. Jacob and K. Müllen, *Macromolecules*, 2006, **39**, 5213–5221.
50 B. N. Boden, K. J. Jardine, A. C. W. Leung and M. J. MacLachlan, *Org. Lett.*, 2006, **8**, 1855–1858.
51 M. J. D. Bosdet, C. A. Jaska, W. E. Piers, T. S. Sorensen and M. Parvez, *Org. Lett.*, 2007, **9**, 1395–1398.
52 Z. Liu and T. B. Marder, *Angew. Chem., Int. Ed.*, 2008, **47**, 242–244.
53 A. J. V. Marwitz, A. N. Lamm, L. N. Zakharov, M. Vasiliu, D. A. Dixon and S.-Y. Liu, *Chem. Sci.*, 2012, **3**, 825–829.
54 A. J. V. Marwitz, M. H. Matus, L. N. Zakharov, D. A. Dixon and S.-Y. Liu, *Angew. Chem., Int. Ed.*, 2009, **48**, 973–977.
55 A. Iida, A. Sekioka and S. Yamaguchi, *Chem. Sci.*, 2012, **3**, 1461–1466.
56 K. Parab, K. Venkatasubbaiah and F. Jäkle, *J. Am. Chem. Soc.*, 2006, **128**, 12879–12885.
57 G. He, N. Yan, H. Cui, T. Liu, L. Ding and Y. Fang, *Macromolecules*, 2011, **44**, 7096–7099.
58 D. T. McQuade, A. E. Pullen and T. M. Swager, *Chem. Rev.*, 2000, **100**, 2537–2574.
59 S. Yamaguchi, T. Shirasaka, S. Akiyama and K. Tamao, *J. Am. Chem. Soc.*, 2002, **124**, 8816–8817.

 This journal is © The Royal Society of Chemistry 2018